

Lanthipeptides

An Amphipathic Alpha-Helix Guides Maturation of the Ribosomally-Synthesized Lipolanthines

Vincent Wiebach, Andi Mainz, Romina Schnegotzki, Mary-Ann J. Siegert, Manuela Hügelland, Nicole Pliszka, and Roderich D. Süßmuth*

Abstract: The recently discovered strongly anti-Gram-positive lipolanthines represent a new group of lipidated, ribosomally synthesized and post-translationally modified peptides (RiPPs). They are bicyclic octapeptides with a central quaternary carbon atom (avionin), which is installed through the cooperative action of the class-III lanthipeptide synthetase *MicKC* and the cysteine decarboxylase *MicD*. Genome mining efforts indicate a widespread distribution and unprecedented biosynthetic diversity of lipolanthine gene clusters, combining elements of RiPPs, polyketide and non-ribosomal peptide biosynthesis. Utilizing NMR spectroscopy, we show that a $(\theta xx)\theta xx\theta xx\theta$ ($\theta = L, I, V, M$ or T) motif, which is conserved in the leader peptides of all class-III and -IV lanthipeptides, forms an amphipathic α -helix in *MicA* that destines the peptide substrate for enzymatic processing. Our results provide general rules of substrate recruitment and enzymatic regulation during lipolanthine maturation. These insights will facilitate future efforts to rationally design new lanthipeptide scaffolds with antibacterial potency.

Introduction

Ribosomally synthesized and post-translationally modified peptides (RiPPs) represent a rapidly expanding and structurally diverse group of natural products. They are characterized by ribosomal synthesis of a precursor peptide, which undergoes structural modifications by one or multiple maturation enzymes.^[1] The common feature in RiPP biosynthesis is that the precursor peptide, encoded within the biosynthesis gene cluster (BGC), consists of an N-terminal leader peptide (LP) region, necessary for molecular recognition by the corresponding enzymes, and a C-terminal core peptide (CP) region, which is post-translationally modified.^[1]

[*] V. Wiebach, Dr. A. Mainz, R. Schnegotzki, Dr. M.-A. J. Siegert, M. Hügelland, N. Pliszka, Prof. Dr. R. D. Süßmuth
Institut für Chemie/ Biologische Chemie
Technische Universität Berlin
Straße des 17. Juni 124, 10623 Berlin (Germany)
E-mail: suessmuth@chem.tu-berlin.de

Supporting information and the ORCID identification number(s) for the author(s) of this article can be found under:
<https://doi.org/10.1002/anie.202003804>.

© 2020 The Authors. Published by Wiley-VCH Verlag GmbH & Co. KGaA. This is an open access article under the terms of the Creative Commons Attribution Non-Commercial NoDerivs License, which permits use and distribution in any medium, provided the original work is properly cited, the use is non-commercial, and no modifications or adaptations are made.

How to cite: *Angew. Chem. Int. Ed.* **2020**, *59*, 16777–16785
International Edition: doi.org/10.1002/anie.202003804
German Edition: doi.org/10.1002/ange.202003804

In general, the processed CP is then proteolytically cleaved from the LP and the mature natural product exported out of the cell. At present, > 20 RiPP classes have been described, of which the lanthipeptides represent the largest and most intensively studied group^[2,3] and often show promising bioactivities, e.g., antibacterial (nisin)^[4] or antiviral (labyrinthopeptin).^[5–8] Their unifying feature is the post-translational installation of the thioether-containing amino acids (methyl)lanthionine ((Me)Lan), (methyl)labionin ((Me)Lab) and most recently avionin (Avi, Figure 1a).^[5,9,10] The lanthipeptides can be further divided into four classes, based on their respective modification enzyme(s),^[1] of which class-III (LanKC) and class-IV (LanL) lanthipeptide synthetases each consist of a lyase, kinase and cyclase domain, with the latter either containing (LanL) or lacking (LanKC) a Zn^{II} cofactor (Figure 1c). The multifunctional LanKC and LanL enzymes install thioethers through phosphorylation (kinase activity) of Ser/Thr sidechains and subsequent elimination (lyase activity) yielding dehydroalanine (Dha) or dehydrobutyrine (Dhb), respectively. A subsequent intramolecular Michael-type ad-

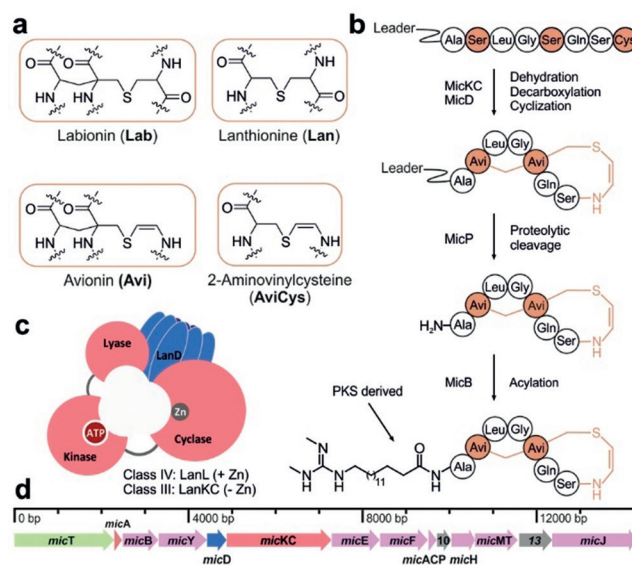


Figure 1. Biosynthesis of lipolanthines. a) Structures of the characteristic amino acids labionin, lanthionine, avionin and aminovinylcysteine occurring in lanthipeptides. b) Microvionin biosynthesis pathway and involved biosynthetic enzymes. c) Schematic representation of tri-modular class-III (LanKC) and -IV (LanL) lanthipeptide synthetases in combination with a cysteine decarboxylase (LanD). d) Microvionin BGC with lanthipeptide-synthetase and precursor peptide genes (coral), cysteine decarboxylase (blue), PKS related genes (purple), and exporter gene (green) highlighted.

dition of a Cys residue to the β -carbon of Dha/Dhb yields Lan/MeLan (cyclase activity), whereas Lab/MeLab is formed, if a second Dha/Dhb is involved.^[1,11,12]

The biosynthesis of certain lanthipeptides requires the additional involvement of a cysteine decarboxylase (LanD), which acts on a C-terminal cysteine, rendering aminovinylcysteine (AviCys) instead of Lan or avionin (Avi) instead of Lab (Figure 1a).^[4,9,13] Interestingly all AviCys- and Avi-containing (lanthi)peptides characterized so far exhibited strong bioactivities, and many have been or still are investigated as drug candidates, such as gallidermin and epidermin (treatment of skin disorders),^[13,14] mutacin B-NY266 (treatment of vancomycin resistant enterococcus, VRE)^[15,16] or microvionin (treatment of methicilin-resistant *Staphylococcus aureus*, MRSA).^[9]

We recently discovered the lipolanthines as a novel type of class-III lanthipeptides with strong anti-MRSA bioactivity. They are bicyclic octapeptides with a central avionin scaffold synthesized from a conserved SxxSxxC motif, and an N-terminal, polyketide synthase (PKS)-derived dimethylguanidino fatty acid (MGFA, Figure 1b). The avionin moiety in microvionin, the first isolated lipolanthine, depends on the cooperative action of the class-III lanthipeptide synthetase MicKC and the cysteine decarboxylase MicD.^[9] The subsequent LP-removal however remained to be investigated, since no corresponding peptidase was identified that could account for LP-removal prior to MGFA attachment.^[9] Many RiPP BGCs do contain dedicated peptidases,^[17] however for class-III and class-IV lanthipeptides the responsible enzymes remained elusive until recently. The Zn-dependent peptidase ApIP, involved in the maturation of the class-III lanthipeptide NAI-112, was shown to have exo- and endopeptidase activity.^[18] Homologous genes were found in all lanthipeptide producers in which they are mostly encoded outside of corresponding BGCs, which is likely also the reason for the missing peptidase gene within the *mic*-BGC. Identification of the responsible peptidases for microvionin biosynthesis is especially important, since LP removal is a prerequisite for MGFA attachment.

A thorough understanding of lipolanthine/lanthipeptide biosynthesis and its regulation is therefore essential to increase production yields and to engineer variants with improved pharmacological properties. The fundamental step in any RiPP maturation is the specific recruitment of the precursor peptide substrate by the modifying enzyme(s) through molecular recognition of the cognate LP.^[19,20] Recent studies have already addressed some aspects of LP recognition in various classes of prokaryotic RiPPs.^[20,21] This led to the proposal of designated RiPP precursor peptide recognition elements (RREs) in multiple modifying enzymes (e.g., lasso peptides, linear-azoline containing peptides and thiopeptides).^[21] For lanthipeptides however, only the dehydratase NisB (Nisin) has been experimentally shown to contain an RRE, which recognizes a conserved F-D/N-L-N/D motif found in various class-I lanthipeptide LPs, whereas no RRE was identified in class-II, -III or -IV lanthipeptide systems yet.^[10,21] Even though earlier studies suggested that the LPs of class-I lanthipeptides adopt a helical structure,^[22] the recent crystallization of the dehydratase NisB (nisin) together with

the corresponding precursor peptide NisA revealed the LP to adopt a β -strand conformation instead, in which it binds to and thus extends an existing three-stranded antiparallel β -sheet in NisB.^[23] For class-III lanthipeptides, a conserved N-terminal LLDLQ motif was proposed in the LP of stackeptide and related lanthipeptides,^[24] whereas Müller et al. observed α -helical properties of the labyrinthopeptin precursor peptide by circular dichroism (CD)-spectroscopy, yet only in the presence of trifluoroethanol (TFE), which is known as a strong and non-native helix formation inducer.^[6,25] Hence, knowledge about recognition motifs in LPs in most lanthipeptide classes ultimately lacks conclusive structural data. Herein, we present an in-depth study on LP recognition, proteolytic cleavage and enzymatic regulation during processing of lipolanthine precursors with implications for all class-III and -IV lanthipeptides and LanD-dependent systems.

Results and Discussion

Genome Mining for Lipolanthine BGCs

Previous studies on the microvionin biosynthesis revealed eight additional lipolanthine BGCs which indicated two distinct gene cluster subtypes (variation in PKS genes) and led to the isolation of nocavionin from *Nocardia terpenica*.^[9] Based on these results and motivated by the strong antibacterial activity of the lipolanthines, we conducted an exhaustive genome mining to determine the distribution of lipolanthines in actinobacterial genomes. This effort yielded > 80 lipolanthine BGCs (Figure 2a), encompassing 48 unique CP sequences and multiple gene clusters which differ significantly from the previously described subtype I (type-I PKS) and subtype II (single-standing PKS) (Figure 2b).^[9]

The analysis of the CP sequences confirmed the characteristic SxxSxxC motif encoding for the avionin scaffold, as well as a broad sequence diversity, including aromatic as well as charged amino acid (aa) residues (Figure 3a). Moreover, we found CP variants with additional C-terminal residues following the conserved Cys, for which the corresponding BGC subtype, which is prevalent in various *Streptomyces* species, lacks the cysteine decarboxylase (*lanD*) homolog, and thus very likely yields lipolanthines with a labionin instead of an avionin moiety (Table S3 in the Supporting Information, Figure 3a).

Further structural differences comprise the variations of MGFA biosynthesis genes, either encoding single-standing PKS and/or NRPS enzymes, a type-I PKS or a combination of both. We also found diverse tailoring enzymes such as glycosyltransferases, cytochrome P450 monooxygenases and ATP-Grasp domain containing enzymes. Hence, the combination of all these biosynthetic genes suggests the potential to produce lipolanthines with an unprecedented structural diversity (Table S4). Based on these observations, we propose two additional subtypes of lipolanthines: Subtype III encompasses all BGCs lacking the cysteine decarboxylase, whereas subtype IV employs a combination of single-standing PKS proteins and a type-I PKS, which differs from the previously

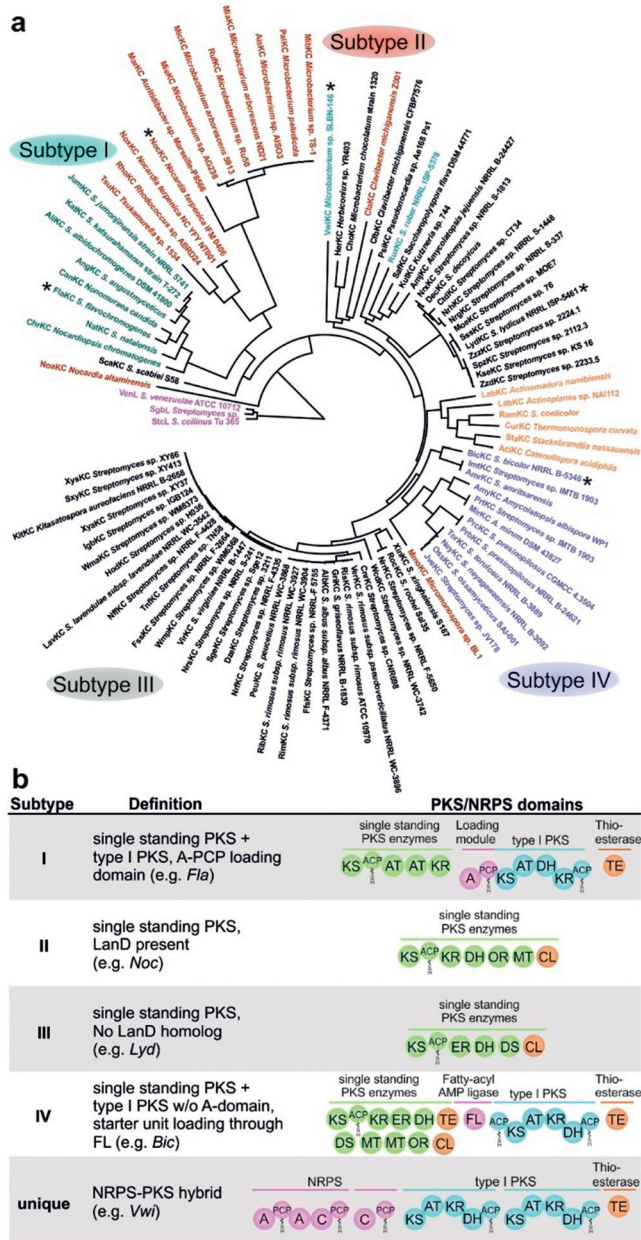


Figure 2. Genome mining of lipolanthines. a) Maximum-likelihood phylogeny of lipolanthines and selected class-III LanKCs (orange) with class-IV LanLs (pink) as the outgroup. Lipolanthine subtypes I (green), II (red), III (black) and IV (blue) and unique BGCs (light blue). Asterisks indicate strains whose PKS systems are depicted in panel (b). S. = *Streptomyces*; A. = *Actinosynnema*; M. = *Microbacterium*; ps. = *pseudoverticillatus*; C. = *Clavibacter* b) Lipolanthine subtypes and examples, defined through the presence of the *lanD* gene and the encoded PKS enzymes. Example PKS domains from all subtypes (Fla, Noc, Lyd, Bic and Vwi) depicted to the right. KS = Ketosynthase; ACP/PCP = Acyl/peptidyl carrier protein; AT = Acyltransferase; KR = Ketoreductase; DH = Dehydratase; TE = Thioesterase; OR = Oxidoreductase; MT = Methyltransferase; CL = CoA-Ligase; ER = Enoylreductase; DS = Desaturase; FL = Fatty-acyl-AMP ligase; A = Adenylation domain; C = Condensation domain.

described system. While subtype-I lipolanthine BGCs encode a type-I PKS with a NRPS-type adenylation (A)-peptidyl carrier protein (PCP) loading domain (predicted to activate

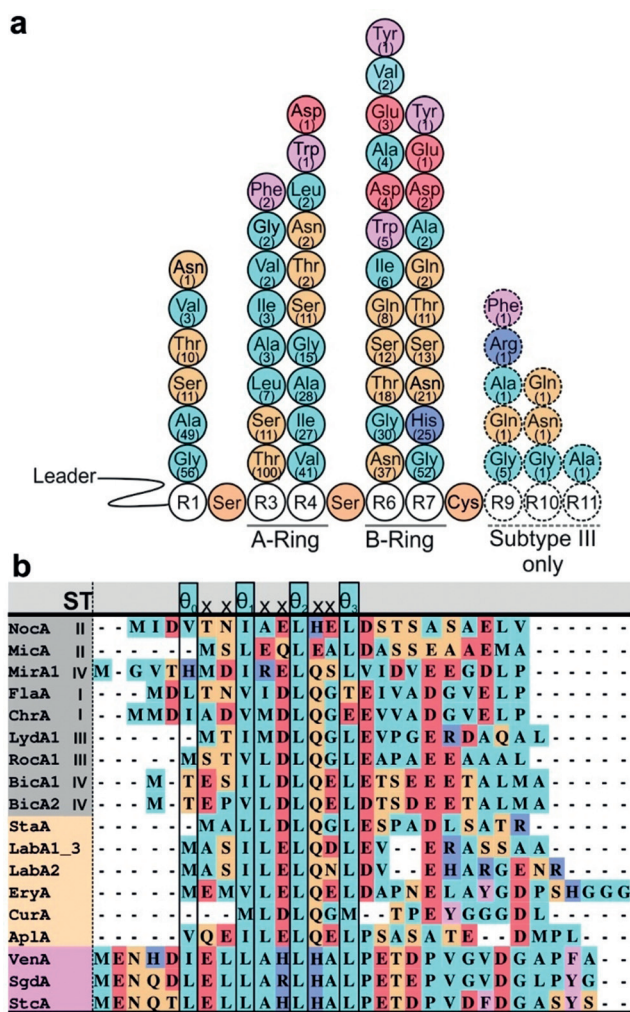


Figure 3. Sequence variations of lipolanthine precursor peptides. a) Amino acid variations within lipolanthine CPs. Numbers indicate the occurrence of an amino acid at this position from all 128 CPs, whereas the color indicates aliphatic (cyan), acidic (red), basic (blue), polar (orange) and aromatic (purple) properties. b) Sequence alignment of selected lipolanthine LPs together with class-III (LabA1-2, StaA, EryA, CurA) and class-IV (VenA, SgdA, StcA) LPs. The conserved $(\theta)_{xx}(\theta)_{xx}(\theta)_{xx}(\theta)$ motif is highlighted. For an extended alignment including all lipolanthine LPs, see Figure S1. ST = Subtype.

guanidinoacetic acid), the newly described lipolanthine subtype IV utilizes a discrete fatty-acyl AMP ligase (FL) instead of an A-domain to load the starting acyl-carrier protein (ACP) of the type-I PKS (Figure 2b).^[26] Finally, two BGCs differed significantly from these subtypes, since they are predicted to employ multidomain NRPS systems to introduce the guanidino moiety (Figure 2b). Taken together these results characterize the lipolanthines as a hybrid of diverse natural product classes, combining biosynthetic features from RiPPs, polyketides, NRPs and polysaccharides. This structural diversity thus offers great prospects for engineering approaches and the discovery of novel lead structures.

Secondary Structure of Lipolanthine LPs

In order to identify potentially conserved recognition motifs, the LP sequences of all putative lipolanthines were aligned with selected class-III and class-IV lanthipeptide LP sequences (Figure 3b and S1). Even though a stretch of seven amino acids is generally well conserved, all investigated LPs share the same $\theta_1xx\theta_2xx\theta_3$ motif, where θ represents an aliphatic aa (I, L, V or M and rarely T, see below) and “x” any canonical aa. For some precursor peptides this sequence is N-terminally elongated thus rendering a $\theta_0xx\theta_1xx\theta_2xx\theta_3$ motif, which is particularly prevalent in LPs of subtype-I lipolanthines and class-IV lanthipeptides (Figure 3b). At the C-terminal θ_3 position, this motif exhibits an even broader aa diversity, also allowing for Thr residues. The above-mentioned results revise the N-terminal **LLDLQ** motif previously proposed by Jungmann et al.^[24] of which only two Leu residues (positions θ_1 and θ_2) are conserved (Figure 3b).

The secondary-structure prediction for the leader peptide of MicA ($MicA_{LP}$) suggested a tendency to adopt an α -helical conformation (Figure S2), in particular involving the conserved $\theta_1xx\theta_2xx\theta_3$ motif. This finding is in agreement with software-based predictions for class-IV lanthipeptides by Hegemann et al., who also suggested the formation of an α -helix within the LP of class-IV lanthipeptides.^[11] To investigate the formation of a recognition α -helix in LanA precursor peptides, $MicA_{LP}$ (*M. arborescens*, microvionin, subtype II), $NocA_{LP}$ (*N. terpenica*, nocavionin, subtype II) and $FlaA_{LP}$ (*Streptomyces (S.) flavochromogenes*, unknown product, subtype I) were chemically synthesized and their secondary structure propensities analyzed by CD and nuclear magnetic resonance (NMR) spectroscopy under various conditions. CD spectroscopy in aqueous solutions revealed that $MicA_{LP}$ partially adopted α -helical conformations coinciding with lower temperatures and lower pH values (Figure S4–5), with a maximal α -helical content of 20% for $MicA_{LP}$ (Table S7). By contrast, $NocA_{LP}$ and $FlaA_{LP}$ exhibited mostly random-coil structures with very limited (3–6%) α -helical contributions (Tables S8–9).

To exactly determine the localization of the predicted α -helix, we analyzed all three LPs in solution at pH 4.5 by means of 2D NMR spectroscopy (see Figure 4, Tables S10–12 and Figures S74–83 for NMR spectra and resonance assignments). For $MicA_{LP}$ a comprehensive analysis of relevant NMR parameters such as chemical shifts δ_{1H} and δ_{13C} , scalar coupling constants $^3J_{HnH\alpha}$, as well as nuclear Overhauser enhancement (NOE) patterns unambiguously identified a two-turn α -helix formed by residues Leu⁻¹⁷ to Asp⁻¹⁰ (Figure 4b). It is important to mention, that this α -helix comprises the conserved $\theta_1xx\theta_2xx\theta_3$ motif and has amphipathic character with residues Leu⁻¹⁷(θ_1), Leu⁻¹⁴(θ_2), Leu⁻¹¹(θ_3) and residues Glu⁻¹⁶, Glu⁻¹³ and Asp⁻¹⁰ representing the hydrophobic and negatively-charged patches of the α -helix, respectively (Figure 4b and S3).

As observed by CD spectroscopy, temperature-dependent NMR experiments likewise demonstrated that the α -helical structure of $MicA_{LP}$ is stabilized at lower temperatures (Figure S74). NMR analysis of both $NocA_{LP}$ and $FlaA_{LP}$ revealed that they are conformationally much less defined

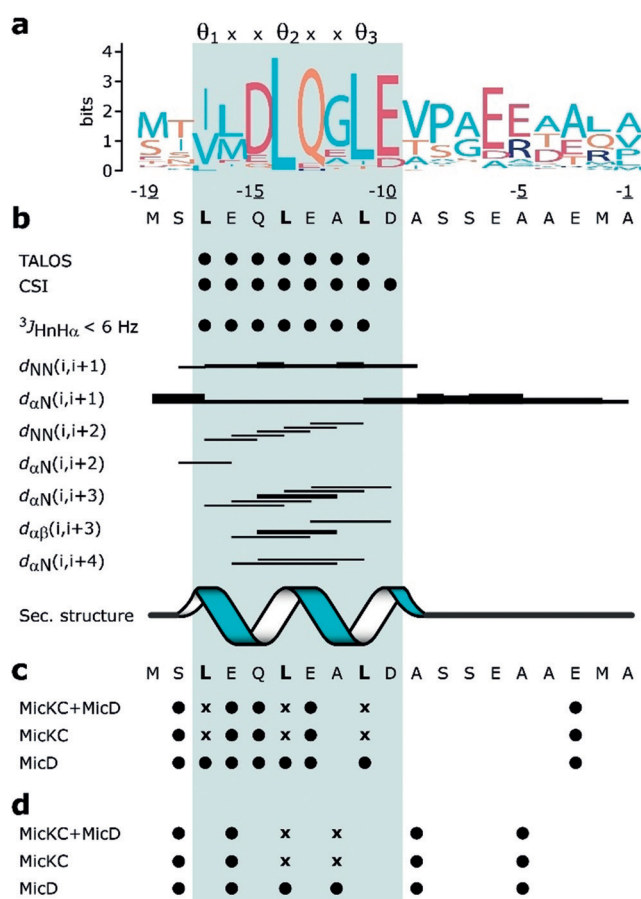


Figure 4. Structural characterization of $MicA_{LP}$. a) Amino acid conservation within all lipolanthine LPs illustrated as a WebLogo.^[27] The $\theta_1xx\theta_2xx\theta_3$ motif is highlighted. b) Summary of NMR parameters relevant for secondary structure assignment of $MicA_{LP}$ at pH 4.5 and 277 K: Analysis of i) Chemical shifts via programs TALOS+^[28] and CSI3.0,^[29] ii) Scalar coupling constants $^3J_{HnH\alpha}$ and iii) characteristic NOE contacts between nuclei H_N , H_α and H_β (d_{XY}). Filled circles indicate α -helical conformation. Rectangles represent dipolar interactions between indicated nuclei of the connected residues with the line-width being inversely proportional to the interatomic distance. The helical segment is shown at the bottom. c)–d) Influence of amino-acid replacements through Ala (c) or Pro (d) in the LP region of MicA on enzymatic processing of its CP. Filled circles indicate no significant changes with respect to wildtype MicA, whereas crosses represent variants for which no avionin formation was observed by MS. The assays have been performed using MicKC and MicD either separately or in combination.

than $MicA_{LP}$. This observation is in agreement with secondary-structure predictions, which indicated the highest α -helical propensity for $MicA_{LP}$ and the lowest for $FlaA_{LP}$ (Figure S2). The overall lower α -helical propensity of $FlaA_{LP}$ may be ascribed to the presence of Gly⁻¹² and β -branched amino acids such as Ile⁻¹⁶ and Thr⁻¹¹ within the $\theta_1xx\theta_2xx\theta_3$ motif (Figure S2).^[30] Nevertheless, secondary structure propensity (SSP) scores,^[31] that rely on chemical shift information and that are very sensitive to small populations of secondary structures within a conformational ensemble, suggested that there is also α -helical propensity for $NocA_{LP}$ again encompassing the $\theta_1xx\theta_2xx\theta_3$ motif (Figure S2). A hypothetical helical-wheel representation of $NocA_{LP}$ shows that its poten-

tial α -helix would also be of amphipathic character, although with a different arrangement of hydrophobic and charged patches compared to MicA_{LP} (Figure S3). In consequence, we postulate that free LanA precursor peptides of lipolanthines are rather flexible in nature with a varying degree of inherent α -helical propensity in the LP region. We suspect that α -helix formation/stabilization may mostly be triggered upon interaction with the binding partner LanKC. If this mechanism is specific for lipolanthines or rather represents a general feature of class-III and -IV lanthipeptides, as unequivocally suggested by sequence conservation (Figure S1), has to be shown in future experiments. Furthermore, the organization of the helical amphipathicity might explain the specific recruitment of precursor peptides to their cognate modifying enzyme (Figure S3) and thus represents an important parameter for rational engineering approaches.

It is noteworthy that the SSP scores for MicA_{LP} indicate an α -helical propensity also C-terminally from the $\theta\text{xx}\theta\text{xx}\theta$ motif (Figure S2) thus potentially extending the α -helix in MicA_{LP} by two additional turns (Leu⁻¹⁷ to Ala⁻⁵). We cannot rule out that MicA would indeed adopt such an elongated α -helix in its complex with MicKC, but sequence alignments for all lipolanthine LPs illustrate a rather high abundance of the α -helix breakers Pro and Gly at positions -8 and -7, respectively (Figure 4a and S1). Furthermore, considering the current knowledge of domain-domain arrangements in class-II lanthipeptide synthetases,^[32] we expect that a flexible linker region of only three to four residues between the recognition α -helix and the actual substrate (CP) might be too short to allow for proper substrate shuttling between three catalytic centers with hypothetical distances of about 20–30 Å, as shown for the class-II synthetase CylM (PDB: 5DZT).^[32] This may only be partially compensated by highly mobile LP binding elements in LanKCs, that could basically function as substrate translocators, for example, similar to peptidyl-carrier protein domains in NRPS.^[33] Future structural biology studies on LanKC-LanA complexes may answer these questions.

LP Recognition and Enzymatic Processing of Lipolanthines

Our structural data demonstrate the rather dynamic nature of lipolanthine-LPs and their varying degree of inherent α -helical propensity, which might be exploited upon interaction with the corresponding enzymes. We speculated that stabilization of the α -helix would originate from hydrophobic contributions to the binding energy involving the highly conserved $(\theta\text{xx})\theta\text{xx}\theta\text{xx}\theta$ motif. In order to further confirm our structural model of lipolanthine-LPs and study substrate recognition through MicKC and MicD we performed an Ala scan of the N-terminal region of MicA to disturb its $\theta_1\text{xx}\theta_2\text{xx}\theta_3$ motif, and monitored avionin formation in vitro by means of HR-HPLC-MS to assess the impact on enzymatic processing. In agreement with our in-silico predictions, only MicA variants L⁻¹⁷A (θ_1), L⁻¹⁴A (θ_2), L⁻¹¹A as well as L⁻¹¹E (θ_3) abolished avionin formation (Table S21), whereas all replacements in other positions, including polar and ionic residues (S⁻¹⁸A, E⁻¹⁶A, Q⁻¹⁵A, E⁻¹³A and E⁻³A), had

no significant impact on substrate conversion (Figure 4c). Notably, due to the high preference of Ala to adopt an α -helical conformation,^[30] we expected Ala replacements to stabilize the α -helix in the corresponding MicA variants. The inhibition of avionin formation in the case of Leu \rightarrow Ala variants thus underlines the importance of branched, hydrophobic residues flanking one side of the recognition α -helix, whilst ionic and polar interactions seem to play a minor role for recruitment of the LP to the modifying enzymes (Figure 4c).

To further assess the importance of α -helical properties, we introduced Pro at key positions in the leader region of MicA to diminish α -helix formation. Variations in the central segment of the α -helix of MicA (L⁻¹⁴P and A⁻¹²P) abolished avionin formation, whereas replacements at the ends of the α -helix (S⁻¹⁸P, E⁻¹⁶P and A⁻⁹P) as well as in the linker region

(A⁻⁵P) had no significant impact on substrate conversion (Figure 4d), revealing not only the conserved motif but also the helical structure to be essential for enzymatic conversion.

In order to decode the individual effects of LP variations on MicKC and MicD respectively, we repeated the assays with each enzyme separately, thereby revealing significantly different substrate requirements. While the activity of MicD was unaffected by any amino acid exchange within the LP, the activity of MicKC was abolished, whenever the $\theta\text{xx}\theta\text{xx}\theta$ motif was altered (Figure 4c,d). Only an N-terminal truncation of MicA by six amino acids impeded decarboxylation by MicD (Table S21). The inhibition of avionin formation, observed in the combined MicKC-MicD reactions (Figure 4c,d), can therefore directly be attributed to the requirements of MicKC towards its cognate LP. Considering that LanD enzymes, for example, EpiD involved in epidermin biosynthesis,^[34] generally exhibit a limited specificity towards their substrates (high yield of reactive enethiol-intermediates),^[13] it stands to question how efficient catalytic turnover is regulated and formation of unspecific side-products is prevented. The comparison of single and combined reactions indicates that the activity of MicD is regulated by MicKC, even if MicKC is incapable of converting the substrate (Figure 4c,d and S20–39). To further decode these substrate requirements we performed an Ala-scan of the CP revealing the C-terminal Cys as essential for conversion by either enzyme, whereas MicD exhibited additional specificity for the CP length, hence not accepting any amino acid introductions (Table S22). Furthermore, the acceptance of a Ser²Thr variant suggest the potential for methyl-avionin formation. At last, MicKC was able to dehydrate various CP variants, only being effected by exchanges of Ser⁵ or Cys⁸ involved in B-ring formation (Table S22, Figure S41–51).

To further analyze these effects, the reactions with MicA were quenched at different time points. In the MicD-only and MicKC/MicD-coupled reactions, nearly all MicA was converted after 2.5 h. By contrast, a significant amount of Dha formation was only observed in MicKC-only reactions after an extended incubation time of > 10 h (Figure S17–19). These results suggest a mutual regulatory mechanism in which the catalytic activity of MicKC is significantly triggered in the presence of MicD. On the other hand, MicD is fully active alone in vitro, yet its activity is controlled by MicKC—

either through allosteric effects or substrate control (Figure 4c,d).

Intrigued by the mutual regulation of LanKC and LanD enzymes and the genome mining results, we cloned and investigated three further lipolanthine systems, namely FlaKC/FlaD (subtype I, *S. flavochromogenes*), the BicKC/BicD system (subtype IV, *S. bicolor*) and the LanD-independent LydKC (subtype III; *S. lydicus*) to obtain further insight into lipolanthine biosynthesis. Incubation of FlaA together with FlaKC and FlaD resulted in avionin formation, whereas FlaKC was inactive in the absence of its partner enzyme (Table 1, Figure S65). Similar to MicKC, BicKC alone was only partially able to dehydrate its precursor peptides BicA1 and BicA2 (Figure S52–53) (Table 1). Avionin formation through BicKC/BicD was observed for both precursor peptides, with Thr⁴ (A-ring) of BicA2 being additionally dehydrated to Dhb, whilst Ser⁴ of BicA1 remained unmodified. Investigation of the LanD-independent LydKC reaction resulted in a mass shift of –54 Da for LydA arising from the formation of Lab and Dhb (Figure S54). As predicted, this system was furthermore able to convert a precursor peptide variant with an additional C-terminal Gly residue (LydA-G⁹), suggesting that larger lipolanthines with more than eight amino acids are accessible with this subtype (Table 1, Figure S55). Finally, we performed assays combining LanD-independent LydKC with other lipolanthine LanDs. However, none of the reactions resulted in avionin formation (Figure S56).

Taken together these results suggest a significant difference between these LanKCs, in which the LanD-independent systems readily produce labionin (and Dhb) in the absence of other enzymes, whereas LanD-dependent LanKCs cannot produce labionin and only are fully active in the presence of their respective partner-LanD, always yielding avionin. Even though previous studies investigated cysteine decarboxylases^[34–36] and multiple crystal structures were obtained,^[13,37,38] so far no conclusive experimental insight into the cooperativity with lanthipeptide synthetases were reported. A previous study on mutacin 1140 biosynthesis showed that a LanD knock-out rendered the formation of lanthionine instead of AviCys.^[39] However, since no quantification or time-depen-

dent analysis was performed this might very well be ascribed to residual activity of the synthetase in the absence of its partner as also observed for MicKC (Figure S17–19), which produced small amounts of Dha and Lan after prolonged incubation with MicA.^[9]

Our findings implicate a high selectivity of LanKCs for their respective LPs, whereas LanD activity is dictated by the CP sequence. To this end, we synthesized hybrid precursor peptides combining LPs and CPs from different lipolanthine systems and investigated the impact on conversion through MicKC/MicD or FlaKC/FlaD (Table S23–24 and Figure S57–72). These results show that both LanDs had high specificity towards the CP sequence, independent of the attached LP. Furthermore, MicKC showed a clear preference for its cognate LP, dehydrating four different attached CPs (MicA_{CP}, TsuA_{CP}, NocA_{CP} and SgeA_{CP}) and rejecting only FlaA_{CP} (Tables S23–24). We could not investigate FlaKC as it is completely inactive in the absence of FlaD.

Proteolytic Degradation of MicA

During RiPP biosynthesis, the LP does not only guide the installation of post-translational modifications (PTMs) through respective modifying enzymes,^[1] but subsequently needs to be proteolytically removed to obtain the mature compound. In lipolanthine biosynthesis this becomes even more essential as the unique lipidation of the avionin moiety requires preceding LP removal (Figure 1b).

Recent studies characterized AplP and related peptidases, which are responsible for LP degradation during the biosynthesis of different class-III and -IV lanthipeptides.^[18,40] These studies proposed a highly conserved (L/V)-(L/F)-(D/E)-L-Q motif as the cleavage site within all class-III and a PDLL motif in class-IV lanthipeptide LPs.^[18,40] However, such a motif is not present in the microvionin LP (see Figure 3b, 4a and S1), but a similar sequence (LEQLE) occurs within the identified $\theta_1xx\theta_2xx\theta_3$ motif. Moreover, we identified two AplP-peptidase homologues, MicP1 and MicP2, in the genome of *M. arborescens*. We therefore set out to investigate if these enzymes also recognize the identified motif and if they are indeed able to fully remove the LP. Hence, we cloned and expressed the genes *micP1* and *micP2*, and investigated the corresponding enzyme activities towards MicA (see SI “peptidase”). Incubations of MicA with either enzyme for 4 h showed similar cleavage patterns, yet revealed a significantly faster cleavage rate for MicP2 (Figure S8), which therefore was chosen for a more detailed characterization. This shows significant differences between MicP2 and other recently characterized peptidases catalyzing LP cleavage in class-IV lanthipeptides,^[40] which are only active after 24 h, following an unknown activation event.

Incubation of MicP2 with MicKC and MicD-processed MicA for 72 h yielded the corresponding avionin-containing CP as a main product, demonstrating that MicP2 was indeed able to fully remove the LP (Figure S10). A shortened incubation time (1 h) yielded a clearly assignable set of proteolytic peptides, which displayed a preferential cleavage C-terminally of acidic residues (especially Glu), and, to

Table 1: Lipolanthine systems and observed modifications installed within the CPs. Dehydration of Thr to Dhb is indicated by an asterisk.

Organism	LanA	Subtype	Core	PTM
<i>S. flavochromogenes</i>	FlaA:	I	ASGSSEGC	Avionin
<i>M. arborescens</i>	MicA:	II	ASLGSQSC	Avionin
<i>S. lydicus</i>	LydA:	III	G*STISGGC	Labionin + Dhb
	LydA-G ⁹		G*STISGGCG	Labionin + Dhb
<i>S. bicolor</i>	BicA1:	IV	ASASSWNC	Avionin
	BicA2:		ASVTSWEC	Avionin + Dhb

a lesser extent, cleavage N-terminally of Ala-Ala motifs (Figure 5b and Figure S13–16). This was further supported by results obtained for the linear mutant peptide MicA-E⁻¹³A, where the introduction of a second Ala-Ala motif clearly altered the cleavage pattern (Figure 5b and Table S14). For some linear peptides, an additional cleavage was observed for example, within the CP (Figure S8–9) and around Ala⁻⁹ (Figure 5b), suggesting a considerably loose substrate specificity rather than a strict adherence to a conserved cleavage site. This stands in opposition to other recently characterized peptidases, which were suggested to adhere to conserved cleavage motifs.^[18,40]

The contradictory cleavage sites between the recently characterized peptidases^[18,40] and MicP2 indicate that, even though related, these peptidases might not share conserved substrate specificities, but rather developed strain-specific cleavage patterns. However, acidic residues are highly prevalent in all class-III and class-IV lanthipeptide LPs (Figure 3b) and appear to represent a more widespread trait of LPs to achieve solubility, recognition and degradation (Figure 6). All recently characterized peptidases^[18,40] produced fragments that could indicate cleavage C- or N-terminally of acidic residues, which were proposed to originate from exopeptidase activity rather than an initial

cleavage event. We however point out that this could also indicate endopeptidase cleavage guided by acidic residues, which has to be investigated in future experiments. Finally, it should be mentioned, that LP sequences appear to have evolved for intrinsic α -helical propensities with limited thermodynamic stability. Such fine-tuned mechanism would allow for an efficient recruitment by modifying enzymes, but would not cause a stable structure free in solution which could hamper proteolytic maturation of modified precursor peptides, in particular of those awaiting N-terminal acylation such as lipolanthines.

Conclusion

Motivated by the strong anti-MRSA activity of microvionin we intended to further investigate this unique compound class. We performed exhaustive genome mining and found a wide distribution of this natural product family within the Actinobacteria. Depending on the presence of a decarboxylase gene *lanD*, as well as PKS and NRPS genes as characteristic features of the BGC, four lipolanthine subtypes (I–IV) have been proposed, containing large BGCs and various additional tailoring enzymes. Utilizing LanKC and LanD enzymes from all four subtypes, we could generate the first labionin and Dhb containing lipolanthines and investigate the difference between LanD-dependent and -independent systems. Due to the unique biosynthesis pathways combining features of lanthipeptides, polyketides and non-ribosomal peptides, the lipolanthine BGCs represent remarkable hybrids of multiple natural product classes: whilst the CP is RiPP-derived, the assembly of the N-terminal MGFA moiety requires PKS- and NRPS-related enzymes. The presence of additional tailoring enzymes such as glycosyl transferases and cytochrome P450 monooxygenases further expands the expected structural diversity. The ongoing investigation on MGFA biosynthesis and the isolation of further lipolanthines will reveal the extent of structural diversity, enable structure–activity relationship studies and aid with the engineering of “custom” lipolanthines.

Our investigation of LP recognition and precursor-peptide processing by HPLC-MS, CD- and NMR spectroscopy revealed the presence of an amphipathic α -helix within MicA_{LP} involving the (θxx)θxxθxxθ motif. The motif itself is highly conserved in all class-III and -IV lanthipeptide LPs, as can be seen in our extensive sequence comparison (Figure S1). We could show that the corresponding α -helix in MicA_{LP} guides maturation, that is, phosphorylation, elimination and cyclization, by MicKC yet not MicD (Figure 6). Previous studies suggesting the preference of α -helical structures for various LPs only relied on software-based predictions or CD spectroscopy in the presence of high TFE concentrations,^[6,22] known to artificially induce α -helix formation.^[25] Even though the enzyme-bound LP structure awaits support by crystallization of the MicKC-MicA complex, our NMR and CD data provide experimental proof of the α -helical propensities of MicA_{LP} free in aqueous solution without helix inducers like TFE. Notably, we consider the strong conservation of the (θxx)θxxθxxθ motif and the

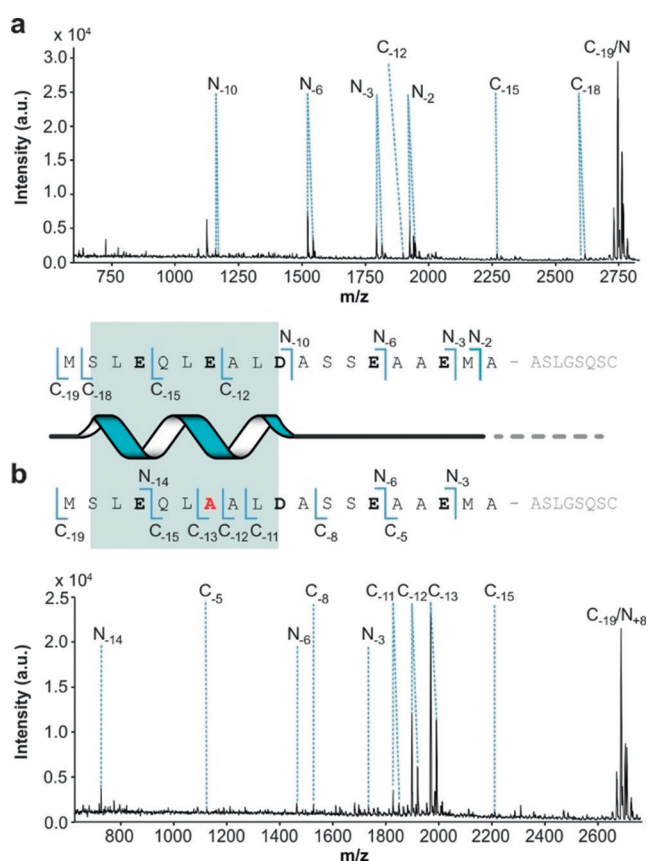


Figure 5. MALDI-TOF-MS-based analysis of MicP2-mediated cleavage of MicA variants, indicating cleavage after Glu and before Ala-Ala motifs. Observed cleavage products of native MicA (a) and MicA-E⁻¹³A (b) after 1 h incubation. The identified α -helix (grey), acidic residues (bold) and the amino acid exchange (red) are highlighted.

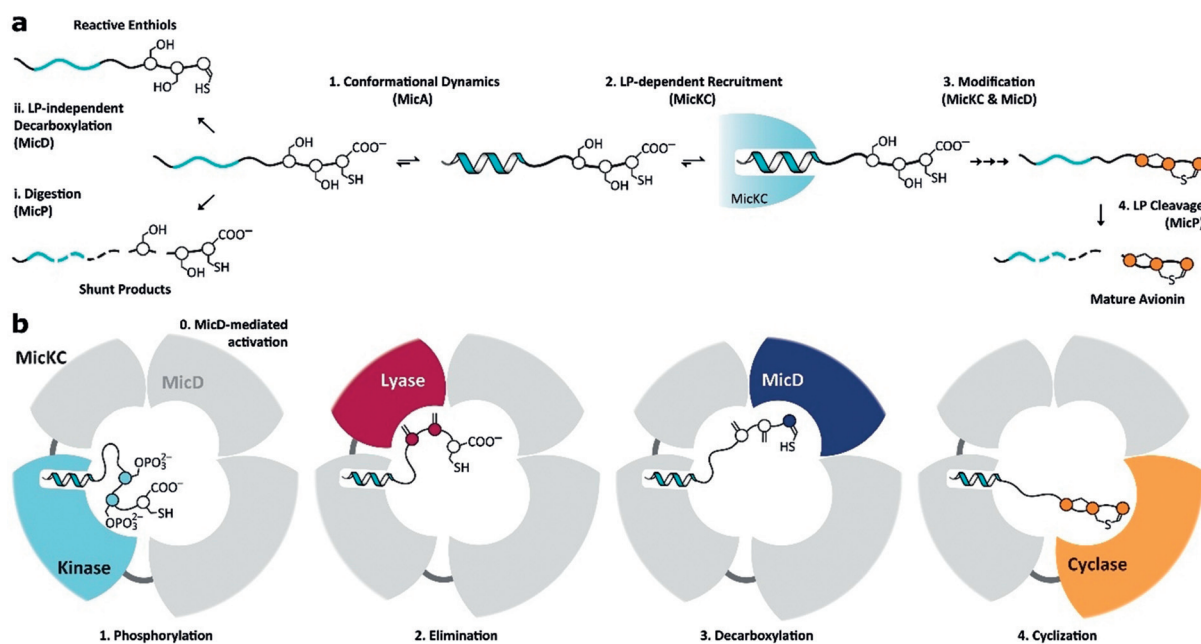


Figure 6. Current model of microvionin biosynthesis. a) The LP-region of MicA undergoes conformational dynamics (1) with the α -helical propensity driving the recruitment to MicKC (2). MicKC also recruits and orchestrates MicD to fully convert the CP of MicA into an avionin scaffold (3, see b). After release from MicKC, the LP of modified MicA again populates unstructured states that are accessible for proteolytic cleavage by MicP (4). The free N-terminus of mature avionin is required for subsequent N-acylation to yield antibacterially active microvionin. The specific LP-dependent recruitment to MicKC protects MicA from premature digestion by MicP and other peptidases (i), as well as from LP-independent decarboxylation by MicD rendering reactive enethiol species (ii). (b) Once MicA is bound to MicKC, a series of well-regulated enzymatic steps is initiated. However, the MicKC-MicA complex appears to be stalled in the absence of MicD and may require allosteric activation (0) through a MicKC-MicD-MicA complex. In this complex, MicKC is capable of phosphorylating (1) and eliminating (2) Ser² and Ser⁵ of the MicA CP, in yet unknown order. Within the MicKC-MicD-MicA complex, MicD decarboxylates MicA in a controlled manner (3) and subsequent cyclization (4) yields the avionin bicycle thereby suppressing any reactive enethiols in the cell.

corresponding amphipathic character of the encoded α -helix (Figure 3, S1 and S3), as a strong argument for its direct involvement in the LanKC-LanA complex. Therefore, it appears very unlikely that the LP adopts a fundamentally different conformation upon binding. Moreover, our findings help to understand the specificities of substrate recruitment and potential cross-talk between non-cognate LanKC-LanA pairs based on the different organization of amphipathicity in the recognition α -helix (Figure S3). We further suggest that in the unbound state, the α -helical structure is only partially populated and thus allows for proteolytic degradation (Figure 6a). Cleavage of the cyclized CP is performed by two Zn-dependent peptidases MicP1 and MicP2, which do not recognize a conserved motif as previously suggested^[18] but, at least in the case of MicP2, cleave C-terminally of Glu distributed throughout the LP. Taken together, these results explain the amphipathic nature of these LPs, in which the conserved, hydrophobic motif is essential for the installation of PTMs, whereas acidic residues guide the subsequent LP removal. Future experiments, including further class-III and -IV lanthipeptide systems, will reveal if this mechanism is specific to microvionin or generally applicable. Finally, we could determine that efficient enzymatic catalysis of avionin formation is based on different substrate requirements and mutual regulation between MicKC and MicD. In our model, catalytic activity of MicD is controlled by MicKC, either allosterically or through substrate control, to avoid formation

of unspecific and reactive side products (Figure 6a). On the other hand, the activity of MicKC is significantly enhanced in the presence of MicD, which implies an allosteric model of a stalled LanKC enzyme being activated by its partner LanD enzyme.

In agreement with the LP-independent, yet CP-specific activity of MicD, this observation hints at a MicKC-MicD complex in which the LP is bound to MicKC, whilst the CP is translocated between catalytic sites of both MicKC and MicD (Figure 6b). In future studies we will address this orchestration of the four catalytic centers in the potential MicKC-MicD complex to understand the catalytic pathway of avionin formation.

In summary, our results shed light on the general principles of substrate recruitment of LanKCs during lipolanthine biosynthesis and their interplay with LanD and LanP enzymes. Owing to the unambiguous sequence alignment of LPs, we believe that these results for MicA and MicKC might be applied to all class-III and class-IV lanthipeptide synthetases. These principles will be essential for any engineering efforts towards biotechnological production of improved lipolanthines/lanthipeptides.

Acknowledgements

This work was funded by the Deutsche Forschungsgemeinschaft (DFG, German Research Foundation) with two grants (RTG 2473 “Bioactive Peptides”, project number 392923329 and project number SU 239/25-1). We additionally thank Pascal Husemann for support in the cloning of the expression vectors. Open access funding enabled and organized by Projekt DEAL.

Conflict of interest

The authors declare no conflict of interest.

Keywords: antibiotics · enzymes · genome mining · lanthipeptides · NMR spectroscopy

-
- [1] P. G. Arnison, M. J. Bibb, G. Bierbaum, A. A. Bowers, T. S. Bugni, G. Bulaj, J. A. Camarero, D. J. Campopiano, G. L. Challis, J. Clardy, et al., *Nat. Prod. Rep.* **2013**, *30*, 108–160.
- [2] M. A. Skinnider, C. W. Johnston, R. E. Edgar, C. A. Dejong, N. J. Merwin, P. N. Rees, N. A. Magarvey, *Proc. Natl. Acad. Sci. USA* **2016**, *113*, E6343–E6351.
- [3] L. M. Repka, J. R. Chekan, S. K. Nair, W. A. van der Donk, *Chem. Rev.* **2017**, *117*, 5457–5520.
- [4] C. Chatterjee, M. Paul, L. Xie, W. A. van der Donk, *Chem. Rev.* **2005**, *105*, 633–683.
- [5] K. Meindl, T. Schmiederer, K. Schneider, A. Reicke, D. Butz, S. Keller, H. Gühring, L. Vértesy, J. Wink, H. Hoffmann, et al., *Angew. Chem. Int. Ed.* **2010**, *49*, 1151–1154; *Angew. Chem.* **2010**, *122*, 1169–1173.
- [6] W. M. Müller, P. Enslé, B. Krawczyk, R. D. Süßmuth, *Biochemistry* **2011**, *50*, 8362–8373.
- [7] G. Férrir, M. I. Petrova, G. Andrei, D. Huskens, B. Hoorelbeke, R. Snoeck, J. Vanderleyden, J. Balzarini, S. Bartoschek, M. Brönstrup, et al., *PLoS One* **2013**, *8*, e64010.
- [8] H. Prochnow, K. Rox, N. V. S. Birudukota, L. Weichert, S.-K. Hotop, P. Klahn, K. Mohr, S. Franz, D. H. Banda, S. Blockus, et al., *J. Virol.* **2019**, *94*, e01471-19.
- [9] V. Wiebach, A. Mainz, M.-A. J. Siegert, G. Lesquame, S. Tirat, A. Dreux-Zigha, J. Aszodi, D. Le Beller, R. D. Süßmuth, *Nat. Chem. Biol.* **2018**, *14*, 652–654.
- [10] W. A. van der Donk, S. K. Nair, *Curr. Opin. Struct. Biol.* **2014**, *29*, 58–66.
- [11] J. D. Hegemann, W. A. Van Der Donk, *J. Am. Chem. Soc.* **2018**, *140*, 5743–5754.
- [12] M. Iorio, O. Sasso, S. I. Maffioli, R. Bertorelli, P. Monciardini, M. Sosio, F. Bonezzi, M. Summa, C. Brunati, R. Bordoni, et al., *ACS Chem. Biol.* **2014**, *9*, 398–404.
- [13] C. S. Sit, S. Yoganathan, J. C. Vederas, *Acc. Chem. Res.* **2011**, *44*, 261–268.
- [14] R. R. Bonelli, T. Schneider, H. G. Sahl, I. Wiedemann, *Antimicrob. Agents Chemother.* **2006**, *50*, 1449–1457.
- [15] D. Field, P. D. Cotter, C. Hill, R. P. Ross, *Front. Genet.* **2015**, *6*, 1–8.
- [16] M. Mota-Meira, H. Morency, M. C. Lavoie, *J. Antimicrob. Chemother.* **2005**, *56*, 869–871.
- [17] E. L. Ongey, P. Neubauer, *Microb. Cell Fact.* **2016**, *15*, 97.
- [18] S. Chen, B. Xu, E. Chen, J. Wang, J. Lu, S. Donadio, H. Ge, H. Wang, *Proc. Natl. Acad. Sci. USA* **2019**, *116*, 2533–2538.
- [19] T. J. Oman, W. A. van der Donk, *Nat. Chem. Biol.* **2010**, *6*, 9–18.
- [20] J. R. Chekan, C. Ongpipattanakul, S. K. Nair, *Proc. Natl. Acad. Sci. USA* **2019**, *116*, 24049–24055.
- [21] B. J. Burkhart, G. A. Hudson, K. L. Dunbar, D. A. Mitchell, *Nat. Chem. Biol.* **2015**, *11*, 564–570.
- [22] A. G. Beck-Sickinger, G. Jung, *Liebigs Ann. Chem.* **1993**, 1125–1131.
- [23] M. a Ortega, Y. Hao, Q. Zhang, M. C. Walker, W. a van der Donk, S. K. Nair, *Nature* **2015**, *517*, 509–512.
- [24] N. A. Jungmann, E. F. Van Herwerden, M. Hügelland, R. D. Süßmuth, *ACS Chem. Biol.* **2016**, *11*, 69–76.
- [25] K. Xiong, S. A. Asher, *Biochemistry* **2010**, *49*, 3336–3342.
- [26] K. Priyadarshan, R. Sankaranarayanan, *J. Indian Inst. Sci.* **2018**, *98*, 261–272.
- [27] G. E. Crooks, G. Hon, J. M. Chandonia, S. E. Brenner, *Genome Res.* **2004**, *14*, 1188–1190.
- [28] Y. Shen, F. Delaglio, G. Cornilescu, A. Bax, *J. Biomol. NMR* **2009**, *44*, 213–223.
- [29] N. E. Hafsá, D. Arndt, D. S. Wishart, *Nucleic Acids Res.* **2015**, *43*, W370–W377.
- [30] C. Nick Pace, J. Martin Scholtz, *Biophys. J.* **1998**, *75*, 422–427.
- [31] J. A. Marsh, V. K. Singh, Z. Jia, J. D. Forman-Kay, *Protein Sci.* **2006**, *15*, 2795–2804.
- [32] S.-H. Dong, W. Tang, T. Lukk, Y. Yu, S. K. Nair, W. A. van der Donk, *eLife* **2015**, *4*, e07607.
- [33] R. D. Süßmuth, A. Mainz, *Angew. Chem. Int. Ed.* **2017**, *56*, 3770–3821; *Angew. Chem.* **2017**, *129*, 3824–3878.
- [34] T. Kupke, C. Kempter, G. Jung, F. Gotz, *J. Biol. Chem.* **1995**, *270*, 11282–11289.
- [35] M. A. Ortega, D. P. Cogan, S. Mukherjee, N. Garg, B. Li, G. N. Thibodeaux, S. I. Maffioli, S. Donadio, M. Sosio, J. Escano, et al., *ACS Chem. Biol.* **2017**, *12*, 548–557.
- [36] F. Majer, D. G. Schmid, K. Altena, G. Bierbaum, T. Kupke, *J. Bacteriol.* **2002**, *184*, 1234–1243.
- [37] M. Blaesse, T. Kupke, R. Huber, S. Steinbacher, *EMBO J.* **2000**, *19*, 6299–6310.
- [38] T. Mo, H. Yuan, F. Wang, S. Ma, J. Wang, T. Li, G. Liu, S. Yu, X. Tan, W. Ding, et al., *FEBS Lett.* **2019**, *593*, 573–580.
- [39] J. Escano, A. Ravichandran, B. Salamat, L. Smith, *Appl. Environ. Microbiol.* **2017**, *83*, e00668-17.
- [40] H. Ren, C. Shi, I. R. Bothwell, W. A. van der Donk, H. Zhao, *ACS Chem. Biol.* **2020**, *15*, 1642–1649.

Manuscript received: March 13, 2020

Revised manuscript received: May 15, 2020

Accepted manuscript online: June 12, 2020

Version of record online: July 24, 2020